The Journal of Chemical Physics

Using isotopologues to probe the potential energy surface of reactions of $C_2H_2^+ + C_3H_4$

Cite as: J. Chem. Phys. **154**, 124310 (2021); https://doi.org/10.1063/5.0046438
Submitted: 03 February 2021 • Accepted: 12 March 2021 • Published Online: 29 March 2021

James Greenberg, Philipp C. Schmid, James H. Thorpe, et al.

The Journal of Chemical Physics ARTICLE scitation.org/journal/jcp

Using isotopologues to probe the potential energy surface of reactions of $C_2H_2^+ + C_3H_4$

Cite as: J. Chem. Phys. 154, 124310 (2021); doi: 10.1063/5.0046438
Submitted: 3 February 2021 • Accepted: 12 March 2021 •
Published Online: 29 March 2021

James Greenberg,[1,2,a)] Philipp C. Schmid,[1,2,3] James H. Thorpe,[4] Thanh L. Nguyen,[4] Katherine J. Catani,[1,2] Olivia A. Krohn,[1,2] Mikhail I. Miller,[1,2] John F. Stanton,[4] and H. J. Lewandowski[1,2]

AFFILIATIONS

[1] Department of Physics, University of Colorado, 390 UCB, Boulder, Colorado 80309, USA
[2] JILA, National Institute of Standards and Technology and University of Colorado, Boulder, Colorado 80309, USA
[3] I. Physikalisches Institut, Universität zu Köln, Zülpicher Str. 77, 50937 Köln, Germany
[4] Quantum Theory Project, Departments of Chemistry and Physics, University of Florida, Gainesville, Florida 32611, USA

[a)] **Author to whom correspondence should be addressed:** jagr3084@colorado.edu

ABSTRACT

Investigations into bimolecular reaction kinetics probe the details of the underlying potential energy surface (PES), which can help to validate high-level quantum chemical calculations. We utilize a combined linear Paul ion trap with a time-of-flight mass spectrometer to study isotopologue reactions between acetylene cations ($C_2H_2^+$) and two isomers of C_3H_4: propyne (HC_3H_3) and allene ($H_2C_3H_2$). In a previous study [Schmid *et al.*, Phys. Chem. Chem. Phys. **22**, 20303 (2020)],[1] we showed that the two isomers of C_3H_4 have fundamentally different reaction mechanisms. Here, we further explore the calculated PES by isotope substitution. While isotopic substitution of reactants is a standard experimental tool in the investigation of molecular reaction kinetics, the controlled environment of co-trapped, laser-cooled Ca^+ ions allows the different isotopic reaction pathways to be followed in greater detail. We report branching ratios for all of the primary products of the different isotopic species. The results validate the previously proposed mechanism: propyne forms a bound reaction complex with $C_2H_2^+$, while allene and $C_2H_2^+$ perform long-range charge exchange only.

I. INTRODUCTION

Small organic carbocations and their neutral counterparts are some of the basic building blocks in organic chemistry and are found in a plethora of chemical environments. For example, acetylene (C_2H_2) has been observed in the interstellar medium (ISM),[2] where it likely plays a central role in the formation of complex organic molecules through condensation reactions.[3–5] Acetylene cations ($C_2H_2^+$) within the ISM are also very likely part of that same story, as it is produced by reactions with smaller [higher ionization potential (IP)] cations or direct ionization from starlight.[6] Characterization and laboratory exploration of such reaction mechanisms can help to explain the vast diversity of complex organic matter observed in the ISM.[7] Apart from C_2H_2 and $C_2H_2^+$, propyne and allene (C_3H_4) are also expected to play a role in the carbon chemical network, leading to the growth of complex molecules in space.[8] Small carbonaceous species are also found in planetary atmospheres, and their gas-phase reactions are believed to be a major source for particulate formation. Specifically, C_3H_4 was recently detected in the atmosphere of Saturn's moon, Titan, and posited to be involved in the formation of tholins that make up its dense haze layer.[9] Furthermore, all three reactants are common in fuels, which has prompted many studies on their chemistry within flames.[10–13] Our study aims to add insight into the fundamental mechanisms involved in the gas-phase bimolecular reaction between $C_2H_2^+$ and two isomers of C_3H_4. Reaction mechanisms elucidated from these studies may also apply to similar carbocation systems in the various environments mentioned above.

Linear Paul ion traps (LITs) have proven to be fruitful environments to study the underlying mechanisms of gas-phase ion–neutral reactions in detail.[14,15] In particular, laser-cooled atomic ions can be used to sympathetically cool co-trapped molecular ions to

translational temperatures below 10 K, thus forming a Coulomb crystal structure. Furthermore, LITs have the ability to purify reactants using radio frequency (RF) secular excitation, which enables mass-dependent ejection of ions from the trap.[16–18] By exposing the two-component Coulomb crystal to a neutral reactant gas, chemistry can be observed to occur at very low concentrations (~10^6 cm^{-3}) and low reaction rates,[19] down to the single atom level.[20]

In addition to the ability to create clean, cold molecular ion samples, the LIT offers a way to determine the reaction products by mass spectrometry. Recently, reaction studies in the Coulomb crystal environment have been improved by radially coupling a time-of-flight mass spectrometer (TOFMS) to the LIT.[21–26] The low translational kinetic energies provide the initial conditions necessary for high mass resolution with $\frac{m}{\Delta m} > 1000$. The TOFMS also detects all constituent masses in the ion trap simultaneously. As reaction product ions are readily co-trapped and sympathetically cooled, one can follow reactions by monitoring the depletion of reactants and the growth of product ions simultaneously. Additionally, the use of Coulomb crystals allows determination of absolute ion numbers.[25] This enables a more complete description of reaction kinetics.

Overall, the degree of control and measurement sensitivity is critical to tracking reaction pathways in the experiment, which allows us to study the kinetics and dynamics of various isotopologue reactions.[27,28] Specifically, following the isotopic distribution of product channels can validate and/or exclude pathways proposed on the basis of potential energy surface (PES) calculations. In related work,[1] we used the tools described above to study the previously unexplored reactions between acetylene cations and two structural isomers of C_3H_4. In the previous experiment, we uncovered isomer dependent reaction mechanisms that govern the reaction. Namely, propyne forms a bound reaction complex with $C_2H_2^+$, while allene and $C_2H_2^+$ perform long-range charge exchange only. As a follow-up, the current article investigates the reaction in further detail by utilizing many isotopologues of the reactants. The kinetics of many isotopic substitutions are characterized and used to explore the validity of the potential energy surfaces presented.

This article describes a detailed investigation into the chemical kinetics of isomer specific chemical mechanisms observed in the reactions of acetylene cations with allene and propyne. After describing the experimental and computational methods, this paper is divided into two major sections: one for reactions involving propyne and another for reactions with allene. Within each section, experimental results are presented first, which includes a model of the observed reaction kinetics and branching ratios for primary products. Second is a description of computational results, specifically, calculations of the relevant potential energy surfaces. Third is a discussion of the experimental results and how the experimental data validate the computational results. Finally, the paper concludes with a summary and an outlook on future work.

II. METHODS

A. Experimental

The details of our LIT-TOFMS apparatus have been described in previous work.[1,25,29–31] We will highlight here the key aspects of the experiment. See Fig. 1 for a schematic layout of the LIT-TOFMS.

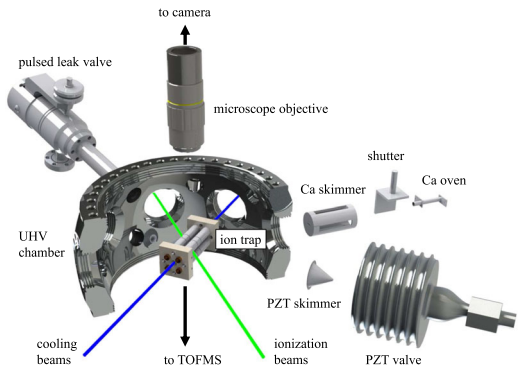

FIG. 1. Schematic representation of the LIT-TOFMS apparatus. A cross-sectional view of the spherical octagon vacuum chamber reveals the ion trap at the center of our experiment. The Ca^+ source is an effusive, skimmed beam of neutral calcium generated by a resistively heated oven. The molecular ion source is a pulsed, skimmed supersonic molecular beam of neutral acetylene seeded in helium. The neutral beams are intersected by pulsed, focused ionization lasers in the center of our trap to load atomic and molecular ions. Ca^+ ions are addressed by continuous-wave diode cooling lasers. A microscope objective outside the UHV chamber is used to image the laser-induced fluorescence from Ca^+. A pulsed leak valve is used to introduce neutral reactants into the UHV chamber. Reproduced with permission from Schmid *et al.*, Phys. Chem. Chem. Phys. **22**, 20303 (2020). Copyright 2020 The Royal Society of Chemistry.

A reaction cycle begins by loading $C_2H_2^+$ ions from neutral molecules delivered into the UHV chamber (~10^{-10} Torr) via a pulsed, skimmed supersonic beam of C_2H_2/C_2D_2 (diluted to ~2% in helium). Acetylene cations are loaded into the trap by the intersection of a focused, pulsed dye laser (LIOP-TEC, 2 mJ/pulse) and the molecular beam at the center of the ion trap. A (1 + 1′) resonance enhanced multiphoton ionization (REMPI) scheme is used at ~216 nm to load $C_2H_2^+$.[32] For $C_2D_2^+$, ~218 nm is used.[33] Both the dye laser and pulsed molecular beam valve are run at a 10 Hz rep rate, which loads hundreds of molecular ions into the trap within a few pulses. This procedure also incorporates many contaminant ions likely due to the high reactivity of acetylene cations and the high laser intensity used. To remove unwanted ions, we implement parametric, resonant, secular mass excitations.[16–18] Quadrupolar excitations of target ion masses are achieved by amplitude modulation (~100 kHz) of the main ion trapping radio frequency (RF). The frequencies of modulations are tuned to eject unwanted masses, thus purifying the acetylene sample for the reaction study. Typically, 150–250 acetylene ions remain in the trap after purification.

Calcium ions (800–1000) are then loaded into the trap and laser cooled to $\lesssim$1 K.[25] The cooled calcium ions sympathetically cool the acetylene ions via the Coulomb–Coulomb interaction to similar translational temperatures.[1] This point in a reaction cycle marks the initial condition (time t = 0) for reaction measurements. See Fig. 2 for a typical, initial, trapped ensemble at t = 0.

The neutral reactant gas is then admitted into the vacuum chamber by a pulsed leak-valve scheme.[29,34] This raises the UHV chamber base pressure of 10^{-10} Torr to a constant reactant gas pressure ($\lesssim 10^{-9}$ Torr) within 2 s, as measured by a Bayard–Alpert

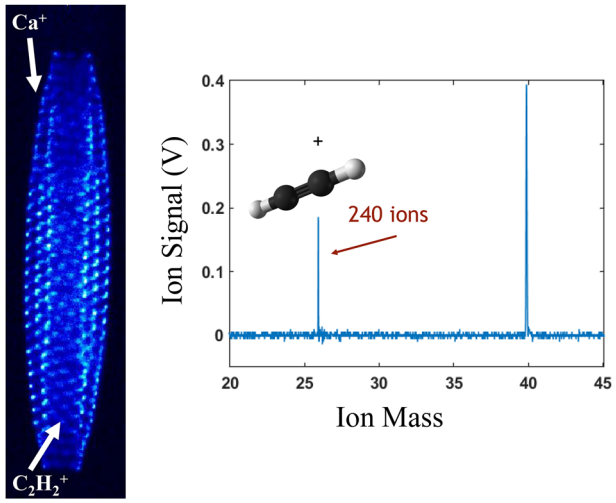

FIG. 2. (Left) False-color fluorescence microscope image of a typical two-component Coulomb crystal (prior to reaction) and its corresponding TOFMS trace (right). The TOFMS data were produced by a single trap loading, i.e., not averaged over multiple experimental cycles. The mass spectrum shows ~240 $C_2H_2^+$ ions co-trapped with ~600 Ca^+ ions.

hot-cathode ionization gauge. The neutral gas is a mixture of allene or propyne diluted in helium (ranging from ~5% to 20%). The room temperature gas reacts with the nearly stationary trapped ions with a translational kinetic energy corresponding to a reaction temperature of ~120 K.[1]

To measure the effects of isotope substituted reactants, deuterium labeled reactants (CDN isotopes, >98% D) are used. For the rest of this paper, we will refer to the explicit chemical formulas of the reactants to emphasize which hydrogen sites were substituted for deuterium. All of the following combinations of acetylene ($C_2H_2^+$ and $C_2D_2^+$), propyne (HC_3H_3, DC_3H_3, HC_3D_3, and DC_3D_3), and allene ($H_2C_3H_2$ and $D_2C_3D_2$) were studied.

After the Coulomb crystal is exposed to the neutral reactant for a variable reaction time of 10–200 s, the pulsed leak valve is closed and the neutral gas is pumped out of the UHV chamber, which quickly (<2 s) returns to the base pressure. Subsequently, the crystal is ejected into the TOFMS to determine the number of ions in the trap and their mass-to-charge ratios. This concludes a reaction cycle. The cycles are repeated 10–15 times per reaction time to build up statistics—simultaneously for the reactants and products. The averaged ion numbers as a function of time map out the reaction kinetics for each pair of isotopologue reactants. Reaction curves and the corresponding analysis are presented in Secs. III A and IV A.

B. Computational

The computational methods for the potential energy surfaces presented in this paper have been discussed in detail in a previous publication and supporting electronic supplementary material.[1] Briefly, the propyne surface was calculated using a hybrid method designated as coupled-cluster single double triple [CCSD(T)]/ANO1//ANO0. This means that molecular geometries and vibrational analysis are obtained using CCSD(T)/ANO0, and then, a single point energy CCSD(T)/ANO1 calculation is performed at this geometry. These results are expected to yield relative energies accurate to within a few kcal/mol (~100 meV). For the allene surface, the mHEAT+[35] method was used to improve the accuracy of the calculations to about ±0.37 kcal/mol (16 meV). The CCSD(T)[36] calculations for the electronic energy done with the ANO0 and ANO1[37] basis sets use the CFOUR program package.[38]

III. PROPYNE—HC_3H_3

A. Experimental results

Over the course of the reaction time, the majority of the trapped acetylene cations reacted away into product ions. From the observed products, a reaction model was built and fit to the reaction data. The model was used to extract reaction rates and primary product branching ratios. In the following, only the results and analysis for the specific isotopologue reaction $C_2H_2^+ + HC_3H_3$ will be described in detail. However, the results of all the isotopologue reactions will be reported. Additional propyne isotopologue data and corresponding analysis can be found in the supplementary material.

The primary product ions for the reaction $C_2H_2^+ + HC_3H_3$ are $C_3H_3^+$, $C_3H_4^+$, and $C_5H_5^+$. Because $C_3H_4^+$ and Ca^+ are both mass 40 u, the two ion species are not readily distinguished from each other in the TOFMS spectra due to the high abundance of Ca^+. The product assignment was directly confirmed by the isotopologue reaction $C_2D_2^+ + DC_3D_3$, which shifted the product $C_3H_4^+$ to $C_3D_4^+$ (mass 44 u) and allowed the product channel to be assigned unambiguously. The product $C_3H_4^+$ can also be inferred by the detection of heavier-mass product ions, $C_6H_5^+$ and $C_6H_7^+$, resulting from the secondary reaction $C_3H_4^+ + HC_3H_3$.[8] These products are second

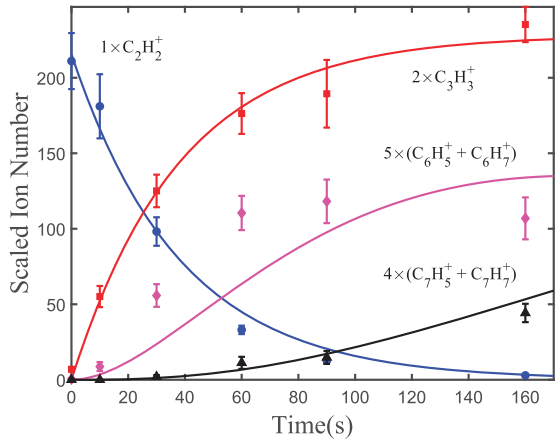

FIG. 3. Example detection of multiple orders of products from $C_2H_2^+ + HC_3H_3$. The product order is apparent by the delay of onset in appearance and a mass that is too large to be a product of $C_2H_2^+ + C_3H_4$. Evidently, $C_3H_3^+$ is first order, $C_6H_5^+$ and $C_6H_7^+$ are second order, and $C_7H_5^+$ and $C_7H_7^+$ are third order. Product channels have been multiplied by a scale factor to enhance clarity of the differences in reaction order. Note that not all measured/modeled product channels are shown in this plot. Solid lines are fits to the reaction model in Eq. (1).

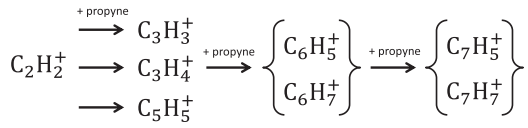

FIG. 4. Reaction model for propyne. Each arrow represents a bimolecular gas-phase reaction between a trapped ion and HC_3H_3. Ions in the same column are of the same reaction order. The exact relationship between higher-order products was undetermined and beyond scope of this work. This ambiguity is represented by the curly brackets.

order in comparison to the primary products because their onset occurs later in time and their mass-to-charge ratio is too large to be a direct product of $C_2H_2^+ + C_3H_4$ (see Fig. 3). Of the three primary order products, only $C_3H_4^+$ was observed to react further with the neutral propyne in excess in the chamber. Tertiary reactions with neutral propyne also occurred, which resulted in product ions $C_7H_5^+$ and $C_7H_7^+$, as shown in Fig. 3. Isotope substituted reactions of higher-order are not the focus of this work. However, the isotope shifts observed for the higher-order product channels confirm higher-order reactions stemmed solely from the product of charge exchange further reacting with propyne.

From the results of $C_2H_2^+ + HC_3H_3$, a reaction model was developed depicting the relationship between the reactant and product ions (see Fig. 4). The large amount of branching in the reaction led to very small ion numbers per product channel, especially for higher-order products. Therefore, detailed relationships between higher-order products were ambiguous and were left as such in the model (represented by curly brackets).

In terms of the reaction, the neutral reactant, propyne, was always considered to be in excess. The pseudo first-order kinetics model leads to a set of differential equations [see Eq. (1)] that were fit to the observed reactant and product ion numbers as a function of time. The following set of equations were derived from the model in Fig. 4:

$$\begin{aligned}
\frac{d[C_2H_2^+]}{dt} &= -(r_{39}+r_{40}+r_{65})[C_2H_2^+],\\
\frac{d[C_3H_3^+]}{dt} &= r_{39}[C_2H_2^+],\\
\frac{d[C_3H_4^+]}{dt} &= r_{40}[C_2H_2^+] - r_{77,79}[C_3H_4^+],\\
\frac{d[C_5H_5^+]}{dt} &= r_{65}[C_2H_2^+],\\
\frac{d[C_6H_5^+ + C_6H_7^+]}{dt} &= r_{77,79}[C_3H_4^+] - r_{89,91}[C_6H_5^+ + C_6H_7^+],\\
\frac{d[C_7H_5^+ + C_7H_7^+]}{dt} &= r_{89,91}[C_6H_5 * + + C_6H_7^+].
\end{aligned} \tag{1}$$

Since the ion numbers were measured explicitly as a function of time, the only fit parameters (r_{39}, r_{40}, r_{65}, $r_{77,79}$, and $r_{89,91}$) are the product channel growth rates in units of s^{-1}.

A critical experimental result is that the total ion numbers are verified to be constant, which indicates that there are no ion losses during the reaction. This was achieved by analyzing the total number of trapped ions as a function of reaction time. The constancy of total ions also solved an experimental inconvenience: the coincidence of $C_3H_4^+$ ions and Ca^+ ions at mass 40 u, which led to issues detecting small numbers of $C_3H_4^+$ ion numbers. In such cases, the number of ions in the mass 40 u channel, not corresponding to Ca^+, was calculated by total ion number conservation, as Ca^+ does not react with propyne (also verified experimentally). The remedy was also applied to all product isotopologues coincident with mass 40 u.

Branching ratios for the primary products $C_5H_xD_y^+$ ($x + y = 5$) and $C_3H_xD_y^+$ ($x + y = 3$) were determined by dividing the respective product growth rates by the total acetylene loss rate. These results are reported as percentages in Table I. The branching ratio of the charge exchange channel can be inferred by subtracting the branching ratios of the two other primary products from 100%. In all models, no H/D exchange was included for the charge exchange channel, $C_3H_xD_y^+$ ($x + y = 4$). The total branching ratios into the primary products do not change much with isotopic substitution. As such, an in-depth discussion of branching in the propyne reaction can

TABLE I. Branching ratios for the $C_3H_xD_y^+$ ($x + y = 3$) and $C_5H_xD_y^+$ ($x + y = 5$) product channels resulting from acetylene cation reactions with propyne. Numbers are the branching ratios (in %) for each mass channel as determined by the fit of the model. Uncertainties are derived from the 90% confidence interval of the rate fits. Blank spaces indicate mass channels not detected in the experiment.

	$C_3H_xD_y^+$ ($x + y = 3$)				$C_5H_xD_y^+$ ($x + y = 5$)					
Formula	$C_3H_3^+$	$C_3H_2D^+$	$C_3HD_2^+$	$C_3D_3^+$	$C_5H_5^+$	$C_5H_4D^+$	$C_5H_3D_2^+$	$C_5H_2D_3^+$	$C_5HD_4^+$	$C_5D_5^+$
Mass (u)	39	40	41	42	65	66	67	68	69	70
$C_2H_2^+ + HC_3H_3$	53(8)				21(5)					
$C_2H_2^+ + DC_3H_3$	24(5)	37(6)			2(4)	18(5)				
$C_2H_2^+ + HC_3D_3$	1(3)	41(5)	17(4)	4(3)			11(3)	7(3)		
$C_2H_2^+ + DC_3D_3$		49(6)	15(4)	11(3)				11(4)	3(3)	
$C_2D_2^+ + HC_3H_3$	24(3)	34(4)	4(2)			3(2)	14(2)			
$C_2D_2^+ + DC_3H_3$	5(3)	51(6)	14(4)	3(3)			5(3)	10(3)		
$C_2D_2^+ + HC_3D_3$		43(5)	15(3)	14(3)					11(3)	2(3)
$C_2D_2^+ + DC_3D_3$		37(7)		29(6)						15(5)

be found in our previous study.[1] Since the neutral reactant density remained roughly constant throughout the reaction, it was also possible to estimate overall reaction rate constants. These are included in the supplementary material, as they are not the main focus of this work.

B. Computational results

The computationally predicted pathway has been discussed in detail in a previous publication and supporting supplementary material.[1] Briefly, the CCSD(T) PES follows a short-range, bound reaction complex (INT0 in Fig. 5). The relevant intermediates, products, and transition states are well below entrance channel energy, and thus, the reaction rapidly flows between the various stationary points on the surface, and nearly complete isotope scrambling is expected. The C_3 and C_5 products of this initial reaction between propyne and acetylene cations match the experimentally observed m/z signal.

C. Discussion

In this section, we discuss how, and to what extent, the results of the propyne isotopologue reactions are consistent with the predictions based on the PES. The most illuminating results that validate the bulk of the proposed PES come from primary product distributions of the isotopologue reactions. The masses observed and those not observed tell a convincing story about the close range interactions between acetylene cations and propyne. Specifically, the distribution of products for the $C_5H_xD_y^+$ $(x + y = 5)$ product channel exhibited all of the isotopic combinations of hydrogen and deuterium possible (see Table I). These H/D scrambled products suggested the formation of a $C_5H_6^+$ complex with a PES conducive to rapid H/D exchange, such as that in Fig. 5. One of many examples of isomerization that leads to exchange can be seen in the ring opening step between INT2 and INT4. The origin of the H/D on the end of the carbon backbone cannot be traced back to either acetylene or propyne. Combined with similar pathways on the PES, any of the hydrogen/deuterium atoms from either reactant could end up in the final product. Because there is only loss of a single hydrogen from the system to form $C_5H_xD_y^+$ $(x + y = 5)$, a maximum of two isotopic arrangements can exist for each isotopologue reaction excluding the fully hydrogenated and deuterated cases (shown in Table I).

The $C_3H_xD_y^+$ $(x + y = 3)$ product distributions complement the results of $C_5H_xD_y^+$ $(x + y = 5)$. We observed all combinations of hydrogen and deuterium allowed by the reactants (see Table I). The combined observations of $C_5H_xD_y^+$ $(x + y = 5)$ and $C_3H_xD_y^+$ $(x + y = 3)$ product channel isotopic distributions validate the proposed PES pathways. Some of the branching ratio confidence intervals include zero. The signal-to-noise ratio of the TOFMS signal for these product channels was good enough to determine they were all, in fact, non-zero. The 90% confidence interval is overly conservative for such small ion numbers, and this result is not a reflection of the model failing.

The experimental results also shed light on the possibility that both long-range and short-range charge exchange could lead to the $C_3H_4^+$ product. By long-range, we mean no bond is formed between reactants in the process of charge exchange. An exclusively long-range charge exchange mechanism would show no signs of H/D scrambling in the isotopic distribution of charge exchange products. By short-range, we mean the $C_5H_6^+$ bound complex (INT0) is formed (see Fig. 5), and the reaction exits the surface via either PRD4 or PRD0, which ultimately produces a $C_3H_4^+$ product. The

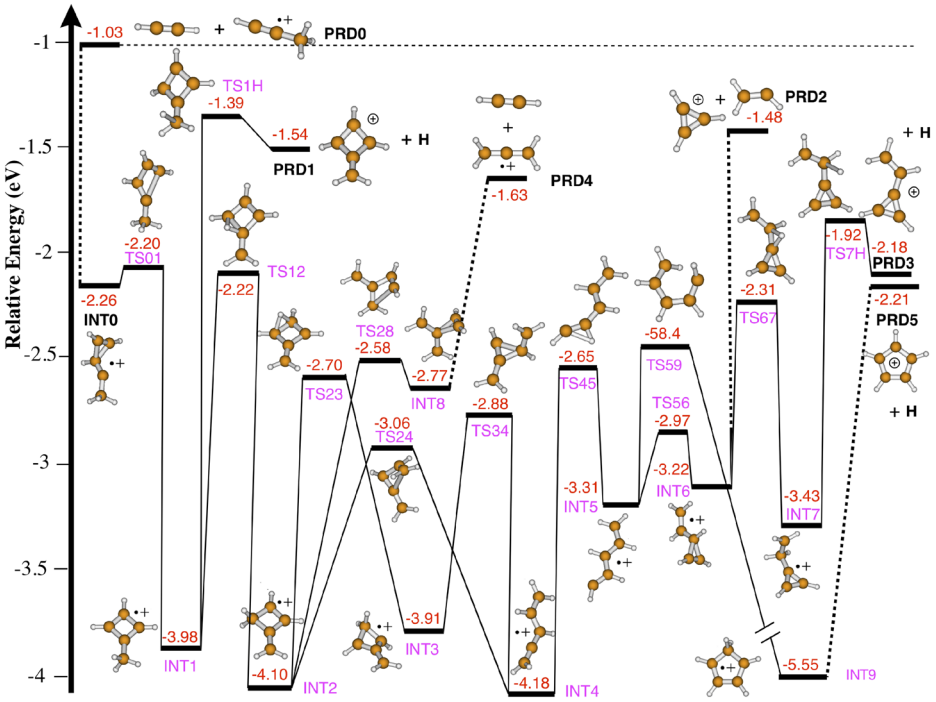

FIG. 5. Potential energy surface (PES) connecting the acetylene cation and propyne to experimentally observed primary products. The energy of each stationary point is calculated using CCSD(T) in the scheme described in the main text. All energies are relative to separated acetylene cation and propyne. Dashed lines between stationary points indicate reactions that occur via a barrierless process. The "●+" symbols on the minima indicate radical cations. Equivalent symbols on transition states are omitted for clarity. Note that the initial point of the PES, PRD0, represents the energy of the reaction after charge exchange has taken place. Reproduced with permission from Schmid *et al.*, Phys. Chem. Chem. Phys. **22**, 20303 (2020). Copyright 2020 The Royal Society of Chemistry.

products would have the possibility to H/D exchange and produce a broad spectrum of isotope-shifted products. We investigated this second possibility by adding isotope-scrambled charge-exchange product channels, $C_3H_xD_y^+$ ($x + y = 4$), to our reaction rate models. In all cases, the rates of the added channels were not statistically different from zero. Additionally, three reactions were measured where such an isotope-scrambled signal should occur in background-free mass channels. Namely, $C_2D_2^+$ with HC_3H_3, DC_3H_3, and HC_3D_3 could result in the products $C_3D_2H_2^+$ (mass 42 u), $C_3D_3H^+$ (mass 43 u), and $C_3D_4^+$ (mass 44 u), respectively. None of these products were observed. These two results suggest that only long-range charge exchange occurs in this system, and if a bond is formed, PRD3: $C_3H_xD_y^+$ ($x + y = 3$) or PRD5: $C_5H_xD_y^+$ ($x + y = 5$) is favored. Notably, this is thermodynamically consistent with the PES.

There is, however, a difference between the experimental results and predictions of the PES. A notable mass 40 u product for both reactions $C_2D_2^+ + DC_3D_3$ and $C_2D_2^+ + HC_3D_3$ exists. In both of these reactions, the product $C_3H_2D^+$ would correspond to mass 40 u but should not be possible because there are not two hydrogens in either reaction. We have gone to considerable effort to track down the identity or origins of this product and believe it to be the result of a neutral gas contaminant, specifically in the deuterium substituted propyne gases. Since the energetic differences for $C_3H_xD_y^+$ ($x + y = 3$) products are negligible compared to the overall exothermicity, one could expect their branching ratios to conform to a random sampling of the available hydrogens and deuteriums from the various isotopologue reactants. In all cases, the observed branching ratios of mass 40 u products from all deuterated propyne gases were larger than such combinatoric expectations. The unknown product was confirmed to come from reactions with acetylene cations (not Ca^+). The unknown product mass was always 40 u without any isotope shift between the two reactions above, and not observed to react further with propyne (or the proposed neutral contaminant). We also performed control experiments using non-diluted samples of the deuterated propyne gases (HC_3D_3 and DC_3D_3). The results were identical product branching ratios to those presented in Table I, which used mixtures diluted in helium. The consistency between those tests rule out contaminants from our gas delivery system and gas mixing procedures. We also observe the contaminant product with reactions with deuterated allene, which will be discussed later in this paper.

Mass 40 u could also conceivably come from the neutral reactant H/D exchange in the lines that deliver the gas to our vacuum chamber (e.g., $DC_3D_3 \rightarrow DC_3D_2H \rightarrow DC_3DH_2$). While we can expect some H/D exchange occurring within the gas delivery lines, its resulting signals are evidently negligible. We see this in the reaction $C_2D_2^+ + DC_3D_3$ (see Table I) where one would expect to see mass 41 u ($C_3HD_2^+$) from a single H/D exchange, but there was no observed product. We would further assume that one H/D exchange should be more likely than two, which would be needed to produce mass 40 u ($C_3H_2D^+$). Thus, H/D exchange of neutral propyne in the gas delivery lines can be neglected in the course of the analysis.

These observations combined lead us to conclude that our deuterated gases contained some contaminant that competed with the $C_2H_2^+ + C_3H_4$ reaction studied in this paper. However, we have deduced enough about the contaminant reaction, particularly from the heavily deuterium substituted reactions, that we are certain the contamination affected only the branching ratios pertaining to mass 40 u. We also remain confident in our assignments of product masses to chemical formulas.

IV. ALLENE—$H_2C_3H_2$

A. Experimental results

The measurements of the reaction of acetylene cations with allene followed the same procedure as described for propyne above. Following the structure of Sec. III, we will describe only the results and analysis for the specific isotopologue reaction $C_2H_2^+ + H_2C_3H_2$ in detail. We also report the results but do not discuss the details of the other isotopolouge combinations measured. As before, additional allene isotopologue data and corresponding analysis can be found in the supplementary material.

The observed primary product ions for the reaction $C_2H_2^+ + H_2C_3H_2$ were $C_3H_3^+$ and $C_3H_4^+$. Compared to the reaction with propyne, $C_5H_5^+$ was notably not observed. In terms of charge exchange, similar to the propyne case, $C_3H_4^+$ and Ca^+ are both mass 40 u, which were not readily distinguished from each other. The assignment of this product could not be directly confirmed by the isotopologue reaction $C_2D_2^+ + D_2C_3D_2$. The lack of build-up of mass 44 u observed is likely due to a smaller rate into the channel than rate out as compared with propyne. The $C_3H_4^+$ charge exchange product was still inferred by the existence of heavier-mass product ions, $C_6H_5^+$ and $C_6H_7^+$. These products were the result of the reaction $C_3H_4^+ + H_2C_3H_2$,[8] and were evidently second order in comparison to the primary products. In addition, they are too massive to be products of $C_2H_2^+ + C_3H_4$ (see Fig. 6). $C_3H_3^+$ was not observed to react further with the neutral allene in excess in the chamber. We also observed tertiary reactions resulting in product ions $C_7H_5^+$ and $C_7H_7^+$. Isotope substituted reactions of higher-order were not

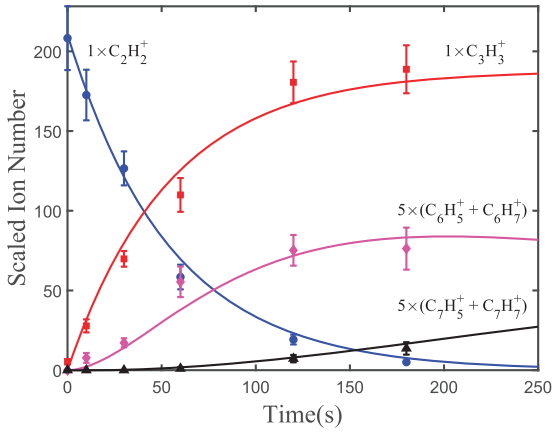

FIG. 6. Detection of multiple orders of products from the reaction $C_2H_2^+ + H_2C_3H_2$. The product order is apparent by the delay of onset in appearance. Additionally, the product masses for secondary and tertiary order products are too heavy to be a product of the bimolecular reaction $C_2H_2^+ + C_3H_4$. Evidently, $C_3H_3^+$ is first order, $C_6H_5^+$ and $C_6H_7^+$ are second order, and $C_7H_5^+$ and $C_7H_7^+$ are third order. Product channels have been multiplied by a scale factor to enhance clarity of the differences in reaction order. Lines are fits to the reaction rate model [Eq. (2)].

the focus of this work. However, the isotope shifts observed for the higher-order product channels confirm higher-order reactions stemmed solely from the product of charge exchange reacting with allene.

As was the case for propyne, the results of $C_2H_2^+ + H_2C_3H_2$ were utilized to develop a reaction model, which depicted the relationship between reactant and product ions (see Fig. 7). Due to product branching, detailed relationships between higher-order products were ambiguous and were left as such in the model (represented by curly brackets). Unlike the propyne case, there was no H/D scrambling for higher-order products, and chemical formulas could be assigned to the products. Nonetheless, precise reactant-to-product relationships for higher-orders were avoided in the model by summing products of higher-orders together.

The pseudo first-order reaction model led to the following set of differential equations [Eq. (2)], in the same way as for the propyne case:

$$\begin{aligned}
\frac{d[C_2H_2^+]}{dt} &= -(r_{39} + r_{40})[C_2H_2^+],\\
\frac{d[C_3H_3^+]}{dt} &= r_{39}[C_2H_2^+],\\
\frac{d[C_3H_4^+]}{dt} &= r_{40}[C_2H_2^+] - r_{77,79}[C_3H_4^+],\\
\frac{d[C_6H_5^+ + C_6H_7^+]}{dt} &= r_{77,79}[C_3H_4^+] - r_{89,91}[C_6H_5^+ + C_6H_7^+],\\
\frac{d[C_7H_5^+ + C_7H_7^+]}{dt} &= r_{89,91}[C_6H_5^+ + C_6H_7^+].
\end{aligned} \tag{2}$$

The ion numbers were measured explicitly as a function of time, leaving the product channel growth rates (r_{39}, r_{40}, $r_{77,79}$, and $r_{89,91}$) as the only fit parameters. Absolute reaction rate constants for each isotopologue reaction are included in the supplementary material.

Branching ratios were determined for the primary product $C_3H_3^+$ in a manner identical to propyne. The results are reported as percentages in Table II. The branching ratio of the $C_3H_4^+$ channel, and its analogous isotopologues, can be inferred by subtracting the branching ratios in Table II from 100%.

B. Computational results

Figure 8 shows the PES of $C_2D_2^+$ and $H_2C_3H_2$ calculated at the mHEAT+ level of theory.[35] In stark contrast to propyne, the only primary product outside of charge exchange was $C_3H_3^+/C_3D_3^+$ with no evidence of H/D scrambling. This suggested that no close

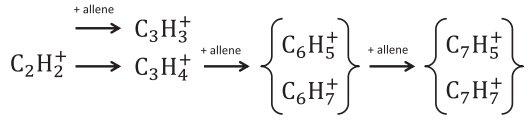

FIG. 7. Reaction model for allene. Each arrow represents a bimolecular gas-phase reaction with a trapped ion and $H_2C_3H_2$. Ions in each column are of the same reaction order. The exact relationship between higher-order products was undetermined and beyond scope of this work. This ambiguity is represented by the curly brackets.

TABLE II. Branching ratios for the isotopologue reactions of acetylene cations and allene. Numbers are the branching ratios (in %) for each mass channel as determined by the fit of the model. Uncertainties are the 90% confidence interval of the branching ratio fit. Blank spaces indicate mass channels not included in the model, as they were not detected in the experiment.

Products	$C_3H_3^+$	$C_3H_2D^+$	$C_3HD_2^+$	$C_3D_3^+$
Mass (u)	39	40	41	42
$C_2H_2^+ + H_2C_3H_2$	90(10)			
$C_2H_2^+ + D_2C_3D_2$		28(7)	6(5)	51(9)
$C_2D_2^+ + H_2C_3H_2$	90(20)			
$C_2D_2^+ + D_2C_3D_2$		20(6)	6(6)	60(10)

range reaction complex between the two species was formed. Otherwise, the reaction would proceed on the identical reaction pathway on the PES of propyne, starting at PRD4, as shown in Fig. 5. This would invariably lead to some $C_5H_5^+$ products and/or isotope scrambling of $C_3H_3^+$ products, similar to propyne. Thus, the allene reaction pathway must be described by a different portion of the full PES than propyne. Zero-point energy corrections were explored for deuterium substitutions on the entire surface, and it was determined that the thermochemistry of the c-$C_3H_3^+$ (PRD1) product channel reaction remains exothermic for any choice of the studied isotopologue reactants.

C. Discussion

We now discuss the experimental results from the allene isotopologue reactions in the context of the PES. The results of the allene isotopologue reactions (see Table II) bolster the mechanism proposed in our previous study: long-range charge exchange, followed by unimolecular decay of the allene cation.[1] Primarily, $C_3D_3^+$ products proceed from reactions with $D_2C_3D_2$, and likewise, $C_3H_3^+$ products follow from $H_2C_3H_2$. The unimolecular decay is mediated by tunneling through the isomerization barrier TS3. While tunneling of a D atom should be much less efficient than an H atom, it is still observed experimentally by the formation of $C_3D_3^+$ (see also TS3 in Fig. 8). We posit that deuterium tunneling is due to the fact that, kinetically, the only other option is vibrational relaxation into $C_3D_4^+$. Given the extremely low background pressure environment, $\lesssim 10^{-9}$ Torr, the vibrationally excited $C_3D_4^+$ would not relax from background gas collisions on a short enough timescale to prohibit tunneling, even for a D atom. We can also conclude that the deuterium tunneling timescale remains shorter than that required to relax via emission of light.

The other two observed products from the reactions with $D_2C_3D_2$, masses 40 u and 41 u, were not predicted by the proposed reaction mechanism. Mass 41 u in its small quantities was very likely the result of neutral reactant contaminants in the form of H/D exchange in the gas delivery lines. Mass 40 u, however, is observed in such abundance that it must be the result of a different neutral contaminant. The product is almost certainly the result of the same contaminant reaction described in Sec. III C. We assume the neutral reactant to be an unidentified contaminant in our $D_2C_3D_2$ sample, as the mass 40 u product does not occur when using the

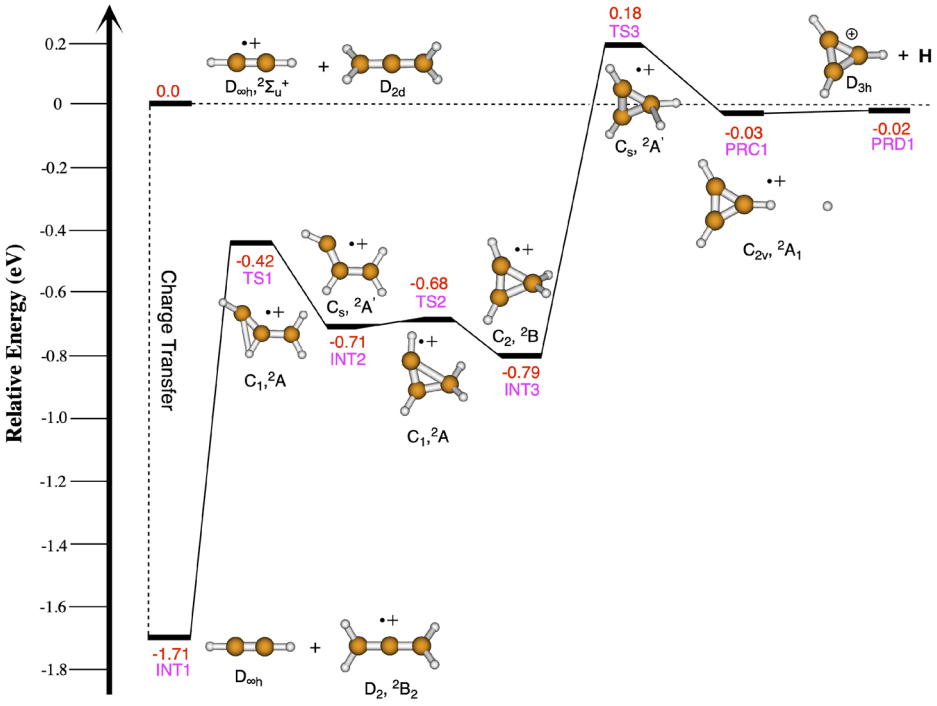

FIG. 8. PES connecting reactants $C_2D_2^+$ and $H_2C_3H_2$ to experimentally observed primary products: $C_3H_3^+$ $C_3H_4^+$. The energy of each stationary point is calculated using the mHEAT+ method.[35] All energies are relative to separated acetylene cations and allene. The "●+" symbols indicate radical cations. Reproduced with permission from Schmid *et al.*, Phys. Chem. Chem. Phys. **22**, 20303 (2020). Copyright 2020 The Royal Society of Chemistry.

$H_2C_3H_2$ sample (see Table II). Neither purification of our neutral gas samples nor further means of identifying the contaminant were available in our current experimental setup. A sufficiently short wavelength vacuum ultra-violet light source[39] could help in future endeavors.

V. SUMMARY AND OUTLOOK

Isotopic substitution is a powerful and well-tested method for gaining insight into chemical reaction processes. We applied this methodology to bimolecular reactions of $C_2H_2^+$ + C_3H_4 in the gas phase in the extremely isolated and specific environment of a Coulomb crystal. For reactions with different isomers of C_3H_4, propyne and allene, branching ratios and isotopic product distributions were measured for the primary products. We determined a fundamentally different mechanism leading to isomer specific reaction products. Together with high-level calculations, we gained understanding into the isomer specific reaction mechanism.

The reaction between acetylene cations and propyne, and their isotopologues, confirms the formation of a bound reaction complex. This complex dissociates into the primary products: $C_3H_3^+$ and $C_5H_5^+$. Meanwhile, the other primary product, charge exchange to $C_3H_4^+$, occurs dominantly from longer range collisions. The results of the isotopologue reactions were used to validate the calculated PES, which demonstrated pathways with extensive H/D exchange.

The reaction between acetylene cations and allene, and their isotopologues, shows only $C_3H_3^+$ as its major product channel without H/D scrambling. This suggested that no short-range reaction complex is formed, but only long-range charge exchange took place. These results are consistent with the calculated PES, which shows that the stable $C_3H_3^+$ product is accessible to it. The energy of the charge-transfer process is converted almost entirely into vibrational energy.

Given the added insight from isotopologue reactions in the current system, this methodology will become an indispensable tool in the characterization of future reactions studied in our ion trap. The ability to unambiguously assign reaction products will aid in modeling reaction pathways contributing to ISM chemistry, interactions in isolated environments, and testing quantum chemical calculations. Further revelations of unique ion–molecule reaction mechanisms will contribute to the basic understanding of how chemical bonds are formed and broken.

In the future, we plan to couple a Stark decelerator to slow the neutral reactant and control the collision energy available for its reaction.[40–42] This will enable reaction dynamics with enhanced energy resolution as compared to the current experiment. Isotopic substitution will be another useful handle in such experiments that allow for precise changes in reaction energetics through zero-point energy corrections. While such changes in energy are typically small, the highly controlled reaction environment of a combined ion trap–Stark decelerator apparatus will have the goal to leverage those changes to do precise thermochemistry measurements; the resulting experiments may set new benchmarks for theory and quantum chemical calculations.

SUPPLEMENTARY MATERIAL

See the supplementary material for additional reaction curves and absolute rate constant estimations.

ACKNOWLEDGMENTS

This work was supported by the National Science Foundation (Grant Nos. PHY-1734006, CHE16-64325, and CHE-1900294), AFOSR (Grant No. FA9550-16-1-0117), and NIST.

DATA AVAILABILITY

The data that support the findings of this study are available from the corresponding author upon reasonable request.

REFERENCES

[1]P. C. Schmid, J. Greenberg, T. L. Nguyen, J. H. Thorpe, K. J. Catani, O. A. Krohn, M. I. Miller, J. F. Stanton, and H. J. Lewandowski, Phys. Chem. Chem. Phys. **22**, 20303 (2020).
[2]J. H. Lacy, N. J. I. Evans, J. M. Achtermann, D. E. Bruce, J. F. Arens, and J. S. Carr, Astrophys. J. **342**, L43 (1989).
[3]T. P. Snow and V. M. Bierbaum, Annu. Rev. Anal. Chem. **1**, 229 (2008).
[4]G. Floyd, R. Prince, and W. Duley, J. R. Astron. Soc. Can. **67**, 299 (1973).
[5]J. S. Knight, C. G. Freeman, M. J. McEwan, V. G. Anicich, and W. T. Huntress, J. Phys. Chem. **91**, 3898 (1987).
[6]A. M. Derkatch, A. Al-Khalili, L. Vikor, A. Neau, W. Shi, H. Danared, M. af Ugglas, and M. Larsson, J. Phys. B **32**, 3391 (1999).
[7]E. Herbst and E. F. van Dishoeck, Annu. Rev. Astron. Astrophys. **47**, 427 (2009).
[8]V. G. Anicich, G. A. Blake, J. K. Kim, M. J. McEwan, and W. T. Huntress, Jr., J. Phys. Chem. **88**, 4608 (1984).
[9]J. H. Waite, D. T. Young, T. E. Cravens, A. J. Coates, F. J. Crary, B. Magee, and J. Westlake, Science **316**, 870 (2007).
[10]P. Weilmünster, A. Keller, and K.-H. Homann, Combust. Flame **116**, 62 (1999).
[11]J. M. Goodings, S. D. Tanner, and D. K. Bohme, Can. J. Chem. **60**, 2766 (1982).
[12]M. Frenklach, Phys. Chem. Chem. Phys. **4**, 2028 (2002).
[13]N. Hansen, J. A. Miller, P. R. Westmoreland, T. Kasper, K. Kohse-Höinghaus, J. Wang, and T. A. Cool, Combust. Flame **156**, 2153 (2009).
[14]B. R. Heazlewood and T. P. Softley, Nat. Rev. Chem. **5**, 125 (2021).
[15]J. Toscano, H. J. Lewandowski, and B. R. Heazlewood, Phys. Chem. Chem. Phys. **22**, 9180 (2020).
[16]J. Schmidt, D. Hönig, P. Weckesser, F. Thielemann, T. Schaetz, and L. Karpa, Appl. Phys. B **126**, 176 (2020).
[17]R. E. March, A. W. McMahon, F. A. Londry, R. L. Alfred, J. F. J. Todd, and F. Vedel, Int. J. Mass Spectrom. Ion Processes **95**, 119 (1989).
[18]M. Welling, H. A. Schuessler, R. I. Thompson, and H. Walther, Int. J. Mass Spectrom. Ion Processes **172**, 95 (1998).
[19]B. R. Heazlewood and T. P. Softley, Annu. Rev. Phys. Chem. **66**, 475 (2015).
[20]A. K. Hansen, M. A. Sørensen, P. F. Staanum, and M. Drewsen, Angew. Chem., Int. Ed. **51**, 7960 (2012).
[21]C. Schneider, S. J. Schowalter, P. Yu, and E. R. Hudson, Int. J. Mass Spectrom. **394**, 1 (2016).
[22]K. A. E. Meyer, L. L. Pollum, L. S. Petralia, A. Tauschinsky, C. J. Rennick, T. P. Softley, and B. R. Heazlewood, J. Phys. Chem. A **119**, 12449 (2015).
[23]S. Jyothi, T. Ray, and S. A. Rangwala, Appl. Phys. B **118**, 131 (2015).
[24]D. Rösch, H. Gao, A. Kilaj, and S. Willitsch, EPJ Tech. Instrum. **3**, 5 (2016).
[25]P. C. Schmid, J. Greenberg, M. I. Miller, K. Loeffler, and H. J. Lewandowski, Rev. Sci. Instrum. **88**, 123107 (2017).
[26]S. Jyothi, K. N. Egodapitiya, B. Bondurant, Z. Jia, E. Pretzsch, P. Chiappina, G. Shu, and K. R. Brown, Rev. Sci. Instrum. **90**, 103201 (2019).
[27]G. K. Chen, C. Xie, T. Yang, A. Li, A. G. Suits, E. R. Hudson, W. C. Campbell, and H. Guo, Phys. Chem. Chem. Phys. **21**, 14005 (2019).
[28]B. R. Heazlewood, A. Tsikritea, L. S. Petralia, J. Loreau, and T. P. Softley, Nat. Commun. **11**, 173 (2020).
[29]P. C. Schmid, M. I. Miller, J. Greenberg, T. L. Nguyen, J. F. Stanton, and H. J. Lewandowski, Mol. Phys. **117**, 3036 (2019).
[30]J. Greenberg, P. C. Schmid, M. Miller, J. F. Stanton, and H. J. Lewandowski, Phys. Rev. A **98**, 032702 (2018).
[31]K. J. Catani, J. Greenberg, B. V. Saarel, and H. J. Lewandowski, J. Chem. Phys. **152**, 234310 (2020).
[32]J. C. Van Craen, M. Herman, R. Colin, and J. K. G. Watson, J. Mol. Spectrosc. **111**, 185 (1985).
[33]A. J. Orr-Ewing, R. A. Morgan, S. H. S. Wilson, C. L. Reed, and M. N. R. Ashfold, J. Chem. Soc., Faraday Trans. **91**, 3327 (1995).
[34]C. Q. Jiao, D. R. A. Ranatunga, W. E. Vaughn, and B. S. Freiser, J. Am. Soc. Mass Spectrom. **7**, 118 (1996).
[35]J. H. Thorpe, C. A. Lopez, T. L. Nguyen, J. H. Baraban, D. H. Bross, B. Ruscic, and J. F. Stanton, J. Chem. Phys. **150**, 224102 (2019).
[36]K. Raghavachari, G. W. Trucks, J. A. Pople, and M. Head-Gordon, Chem. Phys. Lett. **157**, 479 (1989).
[37]L. McCaslin and J. Stanton, Mol. Phys. **111**, 1492 (2013).
[38]D. A. Matthews, L. Cheng, M. E. Harding, F. Lipparini, S. Stopkowicz, T.-C. Jagau, P. G. Szalay, J. Gauss, and J. F. Stanton, J. Chem. Phys. **152**, 214108 (2020).
[39]J. M. Gray, J. Bossert, Y. Shyur, B. Saarel, T. C. Briles, and H. J. Lewandowski, J. Chem. Phys. **154**, 024201 (2021).
[40]Y. Shyur, J. A. Bossert, and H. J. Lewandowski, J. Phys. B: At., Mol. Opt. Phys. **51**, 165101 (2018).
[41]Y. Shyur, N. J. Fitch, J. A. Bossert, T. Brown, and H. J. Lewandowski, Rev. Sci. Instrum. **89**, 084705 (2018).
[42]M. I. Fabrikant, T. Li, N. J. Fitch, N. Farrow, J. D. Weinstein, and H. J. Lewandowski, Phys. Rev. A **90**, 033418 (2014).